

The Formation of Red Copper Glaze in an Oxidizing Atmosphere

Kieu Do Trung Kien^{1,2,*}, Doan Duong Xuan Thuy^{1,2}, Nguyen Vu Uyen Nhi^{1,2}, Do Quang Minh^{1,2,*}

* kieudotruongkien@hcmut.edu.vn & mnh_doquang@hcmut.edu.vn

¹ Department of Silicate Materials, Faculty of Materials Technology, Ho Chi Minh City University of Technology (HCMUT), 268 Ly Thuong Kiet Street, District 10, Ho Chi Minh City, Vietnam

² Vietnam National University Ho Chi Minh City, Linh Trung Ward, Thu Duc City, Ho Chi Minh City, Vietnam

Received: January 2023

Revised: August 2023

Accepted: August 2023

DOI: 10.22068/ijmse.3141

Abstract: This paper introduces a method for producing red copper glaze by adding copper oxide (CuO) and silicon carbide (SiC) additives to the base glaze. SiC created a reducing environment in situ and allowed the glaze to be sintered in an oxidizing furnace environment. Nanocrystals are the determinants of the red color of the glaze. The CuO reduction reaction temperature range of SiC produces a reducing environment in the glaze as detected by the method (DSC). The functional group and phase of nanocrystals were determined by Fourier transform infrared (FT-IR) and X-ray diffraction (XRD) spectroscopy.

Keywords: CuO, SiC, Nanocrystal, In situ reducing agent.

1. INTRODUCTION

Colored glaze containing copper oxide (CuO) used to decorate ceramic products has been widely produced in classical Asian ceramics [1]. In the ionic state, the Cu^{2+} creates a blue-green color, creating the famous celadon in ancient Vietnamese ceramics. When calcined in a reducing atmosphere, the Cu^{2+} ion turns into a metallic copper state, giving a copper-red glaze (when Cu particles are nano-sized) or a thin yellow metal layer on the ceramic surface [2].

In literature, copper-red glaze for ceramics first appeared in China during the Tang Dynasty (618–907 CE) and continued to develop in the Ming Dynasty (1368–1644 CE). The most famous is the blood-red ceramic glaze in Dezhou, Jiangxi province [3]. Ancient Chinese red-glazed pottery is highly valued because of its uniqueness. Ceramic glaze is red like blood, commonly known as cow's blood glaze. This glaze has been fired in a very complex reducing environment, so it always keeps the family secret.

Modern studies on ancient Chinese porcelain have found that the copper-red color is due to nano-sized metallic copper particles [4]. The glaze's red color depends on the nanocrystals' size and content [5, 6]. The red formation of the nanoparticle system is caused by the nanoparticles creating plasmon surfaces and absorbing wavelengths of 500–550 nm. It is not only copper, but other metal particles such as Au, Ag, and Pt with particle sizes in the range of

20–100 nm will also give red color regardless of the chemical nature of the particles [4, 7].

When the glaze containing CuO has fired in a reducing atmosphere, the Cu^{2+} ion was reduced to nano-sized metallic Cu, creating the red glaze. The reducing agent can be CO formed by the kiln air atmosphere when the fuel burns with insufficient oxygen or chemicals mixed in the glaze compositions. The multivalent oxides used as in situ reducing agents for copper-red glazes are usually SnO_2 , CeO_2 [6, 7], and more recently SiC [8–10]. The raw materials supplying Cu for making traditional copper-red glazes are $\text{CuSO}_4 \cdot 7\text{H}_2\text{O}$, CuO, CuCO_3 , $\text{CuCl}_2 \cdot 2\text{H}_2\text{O}$ [11]. In some recent studies, the raw materials used were nano sized CuO [12]. Silicon carbide (SiC) is used industrially as a refractory [13] and a reducing agent in situ at high temperatures in copper-red glazes [5]. The SiC was added in a CuO glaze to reduce in situ agents in the copper-red glazes [14–17].

The advantage of in situ reducing agent SiC is that it can sinter copper red glaze in an oxidizing kiln atmosphere [5, 10]. But for a long firing time, the SiC can be oxidized, and the glaze returns to blue color [7]. Therefore, it is necessary to determine the temperature range and firing time for SiC to create an in situ reducing environment in copper red glaze. The physicochemical changes of high-temperature processes are often studied by differential calorimetry or thermal analysis (DTA/TG or DSC/TG); the Scherrer equation was used to calculate the size of copper crystals

[18-20].

Thus, the reducing environment in the fired process plays a decisive role in the coloration of copper-red glazes. The reduced atmosphere of the firing kiln space creates hazardous environmental problems. The reducing medium in situ is a better application trend because of the firing process in an oxidizing atmosphere. However, using SiC with too much content or inappropriate sintering temperature will be one of the possible causes of glaze surface defects. This defect is formed because the amount of CO₂ produced is too much and cannot escape from the glaze layers.

In this study, fine powders of CuO and SiC were added to the base glaze to give the copper-red glaze. The SiC powder ground is taken from the waste resistor rod and can be in situ reducing agent in the copper red glazes.

2. EXPERIMENTAL PROCEDURES

The base glaze used in these experiments was mixed with the composition (%wt.), including 50% frit (Fritta Company), 30% felspar (India), 10% kaolin (China), and 10% quick lime (Vietnam). Color additives added to the base glaze were 2% (wt.) CuO. The amount of added SiC in the sample was 0, 0.5, 1, 1.5, and 2% by weight, denoted as M01, M02, M03, M04, and M05.

The chemical compositions of the raw materials were analyzed using an X-ray fluorescence (XRF) instrument (ARL ADVANT'X instrument-Thermo Scientific, USA).

Water and carboxymethyl cellulose (CMC) were added to the glaze mixture to form a glaze suspension. The CMC de-flocculant improves the glaze's adhesive properties in green stoneware samples. The water/solid powder ratio was 40/100 (%wt.). The suspension was homogenized by a ball mill in a porcelain jar for 40 mins to obtain the required properties: suspension density from 1.7 to 1.8 g/cm³, the residual amount on the 180-mesh sieve less than 3% (wt.).

The glaze suspension was coated on the surface of the green body samples of 4x4 cm. Then the glazed green body samples were dried in an oven at 120°C for one day. After drying, they were fired in an electric furnace at 1150°C for two hours.

The DSC/TG differential thermal analysis characterized the physicochemical changes occurring during the glaze firing process was

determined by the DSC/TG differential thermal analysis (NETZSCH STA 409 PC/PG device). The M05 sample was chosen for the DSC/TG analysis. The machine operating modes were as follows: The highest temperature at $T_{\max} = 1150^{\circ}\text{C}$, nitrogen gas (N₂) environment, and heating rate 5°C/min. From the TG-DSC analysis results, 1150°C was used as the sample heating temperature.

The fired glaze color was evaluated by the parameter values (L*, a*, b*) in the CIE coordinate system, the device of CR-400/410 Chroma Meter- Konica Minolta, Japan. (CIE stands for Commission Internationale de l'Elclairage. It is also known as the CIE XYZ color space or the CIE 1931 XYZ color space). In which, L*: brightness (from 0-100: dark- light), a*: green (-) - red (+), b*: blue (-) - yellow (+). The cutting surface between the fired stoneware body and its glaze coating was studied with an OLYMPUS optical microscope.

The crystalline phases were investigated by X-ray diffraction (XRD) (device of D2 Phaser device-Brucker, Germany). Analytical conditions on the machine were $K_{\alpha, \text{Cu}} = 1.5406 \text{ \AA}$, $2\theta = 30 - 80^{\circ}$, step of 0.03° . The selected sample is the one with the reddest color. It was already the M5 sample. Determine the existence of structures in the glaze layer by Furrie FT-IR transform infrared spectroscopy (Nicolet 6700 device, Thermo company, USA) with scanning step 0.9643 , scanning angle $400-4000 \text{ cm}^{-1}$.

Based on the XRD diffraction pattern, the crystal size d was calculated according to the Debye-Scherrer formula [18]:

$$d = \frac{K\lambda}{FWHM \cdot \cos\theta} \quad (1)$$

Where d is the crystal size (nm), $K = 0.89$ is the Scherrer coefficient, λ is the wavelength of the X-ray source (1.5406 \AA), $FWHM$ is the widescreeen at $\frac{1}{2}$ diffraction line (rad), θ is the diffraction angle (rad). In this case, the crystal size was calculated at the diffraction peak with the most vigorous intensity, corresponding to the diffraction peak (111).

3. RESULTS AND DISCUSSION

The chemical compositions (%wt.) of raw materials are shown in Table 1.

The chemical compositions (%wt.) of the base glaze after calculating are shown in Table 2.

Table 1. Chemical compositions of raw materials (%wt.)

| | Frit FP 903 | Felspar | Kaolin | CaO |
|--------------------------------|--------------------|----------------|---------------|------------|
| SiO ₂ | 54.40 | 58.66 | 49.54 | - |
| Al ₂ O ₃ | 7.88 | 19.80 | 34.32 | - |
| Fe ₂ O ₃ | 0.12 | - | 1.37 | - |
| MgO | 0.91 | - | - | 0.20 |
| Na ₂ O | 1.02 | 2.87 | - | - |
| CaO | 13.30 | 0.59 | - | 81.27 |
| K ₂ O | 2.90 | 15.64 | 2.46 | - |
| ZnO | 13.70 | - | - | - |
| BaO | 4.80 | - | - | - |
| Other | 0.97 | 2.04 | 0.30 | 0.13 |
| L.O.I. | - | 0.40 | 12.00 | 18.40 |

Table 2. Chemical compositions of the base glaze (%wt.)

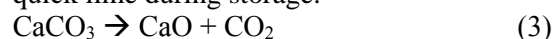
| Oxit | SiO ₂ | Al ₂ O ₃ | Fe ₂ O ₃ | MgO | Na ₂ O | CaO | K ₂ O | ZnO | BaO | Others | L.O.I |
|-------------|------------------|--------------------------------|--------------------------------|------|-------------------|-------|------------------|------|------|--------|-------|
| % | 49.75 | 13.31 | 0.20 | 0.48 | 1.37 | 14.95 | 6.39 | 6.85 | 2.40 | 1.14 | 3.16 |

The physicochemical processes of the mix were determined through the TG-DSC thermal method. Sample M5 was the sample of choice for TG-DSC analysis. The sample M5 was selected for TG-DSC analysis because this was the sample with the highest SiC content. The TG-DSC analysis curve of the M5 sample is shown in Fig. 1. The TG-DSC analysis in Fig. 1 shows that three physicochemical processes occur when sintering glaze mixtures, including frit, felspar, kaolin, CaO, Cu₂O, and SiC. Three thermal effects are recognized clearly on the TG-DSC curve (Fig. 1). These effects include:

- The first thermal effect is in the temperature range from 450 to 600°C. This is an endothermic effect that peaks at 526.7°C. This endothermic peak was accompanied by a weight loss of the sample on the TG line of 0.8%. Many studies on clay minerals have shown that this is the dehydrating process of kaolinite minerals to form meta kaolinite. The decrease in mass corresponds to the loss of H₂O in the reaction (2). This reaction occurs mainly from the presence of kaolinite in the raw material.

$$\text{Al}_2\text{O}_3 \cdot 2\text{SiO}_2 \cdot 2\text{H}_2\text{O} \rightarrow \text{Al}_2\text{O}_3 \cdot 2\text{SiO}_2 + 2\text{H}_2\text{O} \quad (2)$$
- The second thermal effect is in the temperature range from 600 to 800°C. The peak of this endothermic effect is 750.37°C. The endothermic effect with mass reduction is 2.032%. This temperature range corresponds to carbonate decomposition by reaction (3) [21]. This carbonate component is found in kaolinite. Carbonate may also be present in

quick lime material due to the carbonation of quick lime during storage.



- The final endothermic effect is in the temperature range of 1000–1100°C and peaks at 1068.69°C. This thermal effect is the reduction reaction of CuO to Cu under the action of SiC at high temperatures [10]. Reaction (4) demonstrates this reduction. The product of the reaction is Cu. Cu is responsible for the red color of the glaze. However, reaction (4) also produces CO₂. Formed CO₂ can be the cause of defects in the glaze. These defects can be bubbles that form inside or on the surface of the glaze. To solve this problem, the amount of SiC used should not be too much, and the glaze firing temperature should be higher than the reaction temperature 4 (1068.69°C).



Using quick lime instead of calcite is also one of the solutions to the glaze defects. If CaCO₃ is used as a raw material to supply CaO, the CO₂ generated from reaction (3) will increase. This may be the cause of bubbles in the glaze layer. In addition, a large amount of CO₂ can also shift the equilibrium of the reaction (4) from right to left. It prevents reaction (4) from taking place.

TG-DSC results show that above 1068.69°C is the suitable temperature for sintering glaze systems, as shown in Table 1. For the exhausting process to be effective, 1150°C is the selected temperature for sintering glaze systems. Fig. 2 shows glaze samples' images after heating at 1150°C for two hours.

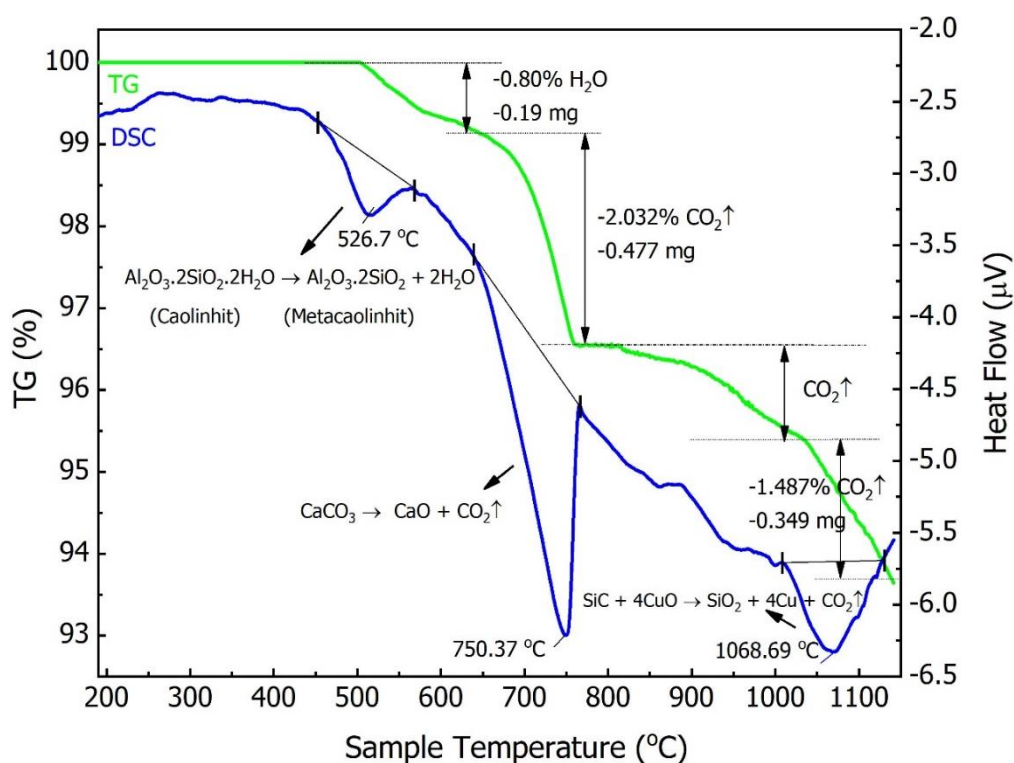


Fig. 1. The TG-DSC analysis curve of the M05 sample

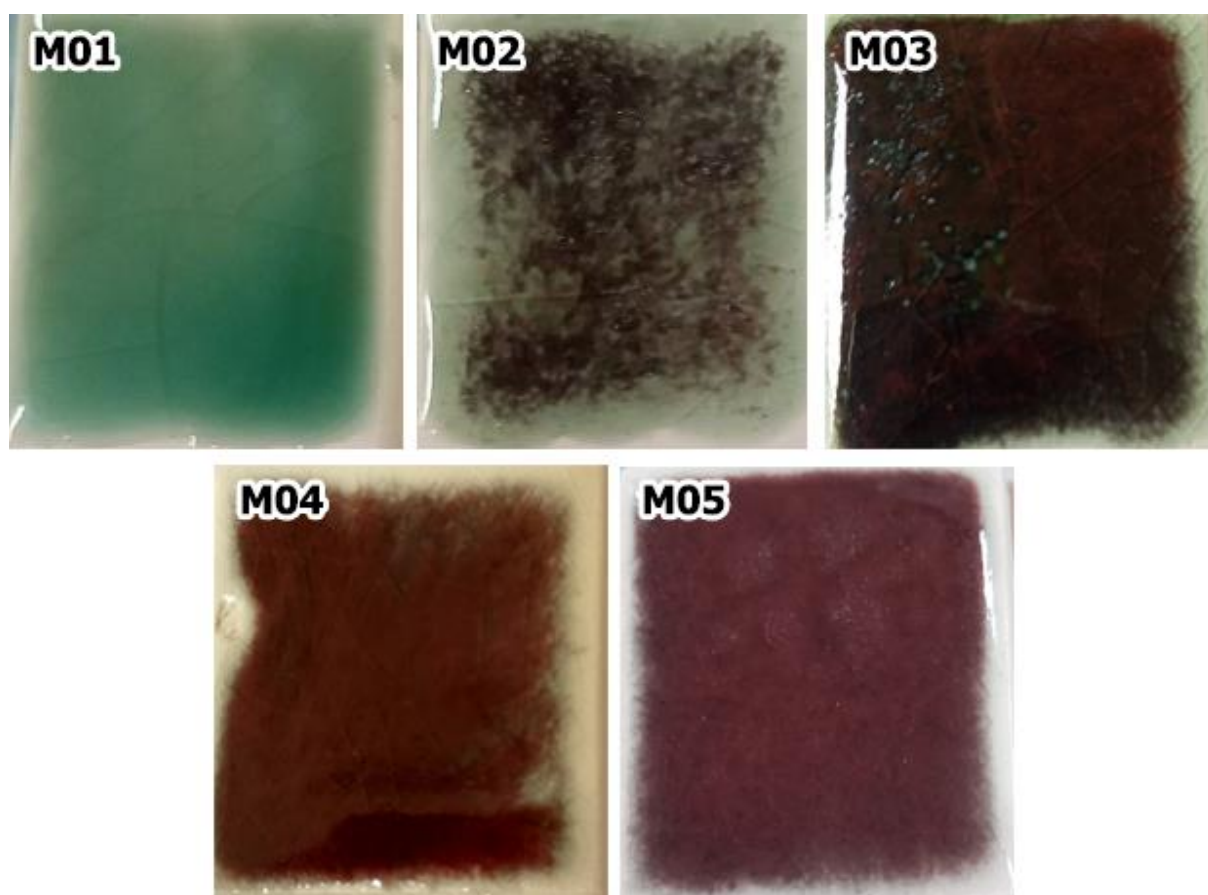


Fig. 2. Images of the M01–M05 samples were sintered at 1150°C for two hours

The samples in Fig. 2 show red glaze as the SiC content gradually increases. Under the same sintering conditions, sample M01 without SiC additive gave the blue color of Cu^{2+} . The sample M05 with the highest SiC content has the most uniform and precise red color. The color of the glazes is also checked through the test of the L^* , a^* , b^* color system parameters. Table 3 shows the samples' L^* , a^* , b^* parameters defined in the CIE coordinate system. Table 3 shows that the color system changes from yellow-green to blood-red when increasing the content of the SiC-reducing agent. This demonstrated the reducing effect of SiC in glazes.

The results also show that the M5 sample, corresponding to 2% SiC is suitable for reducing CuO to form Cu according to the reaction (4). The M5 sample will be used to test the properties of the glaze. Fig. 3 is a cross-section of the M05 sample observed under an optical microscope (5x and 10x magnification). It can see the red color covers the entire thickness of the glaze, even on the undissolved pigment particles. It proves the reducing effect in all glaze volumes. In addition, the optical microscope image makes it easy to observe the intermediate layer formed between the glaze and the ceramic body. This layer proves that the glaze can completely adhere to the ceramic body. Using SiC as a reducing agent did

not affect the adhesion ability of the glaze.

M1 and M5 samples were also investigated by using the XRD method. The XRD analysis results provide information about the phase composition of the glaze. Fig. 4 shows the XRD patterns of the M01 and M05 samples. The results of Figure 4 show that both samples M4 and M5 appear to have the $\alpha\text{-Al}_2\text{O}_3$ mineral (JCPDS# 46-1212). $\alpha\text{-Al}_2\text{O}_3$ is a foreign mineral that occurs in the composition of glaze. $\alpha\text{-Al}_2\text{O}_3$ appears due to mixing in grinding the glaze into powder. So, the XRD analysis shows $\alpha\text{-Al}_2\text{O}_3$ (corundum). The amount of $\alpha\text{-Al}_2\text{O}_3$ mixed in is not significant. However, because the yeast is amorphous, the appearance of $\alpha\text{-Al}_2\text{O}_3$ peaks on the XRD patterns is quite clear. Particularly for sample M5, the glaze sample also appears peaks of Cu (JCPDS# 85-1326) on the XRD pattern. These peaks appear at positions 43.6° , 50.8° , and 74.4° . These peaks show that SiC has reduced CuO to Cu at the sintering temperature of 1150°C .

The formed Cu particle size is also calculated from the XRD pattern using the Debye-Scherrer formula (1). The diffraction peak at position 43.63° , corresponding to the planes with Miller indices (111), is commonly used to calculate the size of copper particles [22]. At position 43.63° in Fig. 5, there is an overlap of Cu and $\alpha\text{-Al}_2\text{O}_3$ peaks.

Table 3. L^* , a^* , b^* values and glaze colors

| Samples | L^* | a^* | b^* | Color |
|---------|-------|--------|-------|--------------|
| M01 | 64.89 | -17.33 | 4.92 | green-yellow |
| M02 | 56.25 | -2.49 | 11.01 | green-yellow |
| M03 | 35.73 | 5.03 | 5.54 | dark red |
| M04 | 32.26 | 9.81 | 9.00 | red |
| M05 | 34.39 | 10.61 | 9.26 | red-blood |



Fig. 3. Optical microscope images of a cross-section of the M05 sample

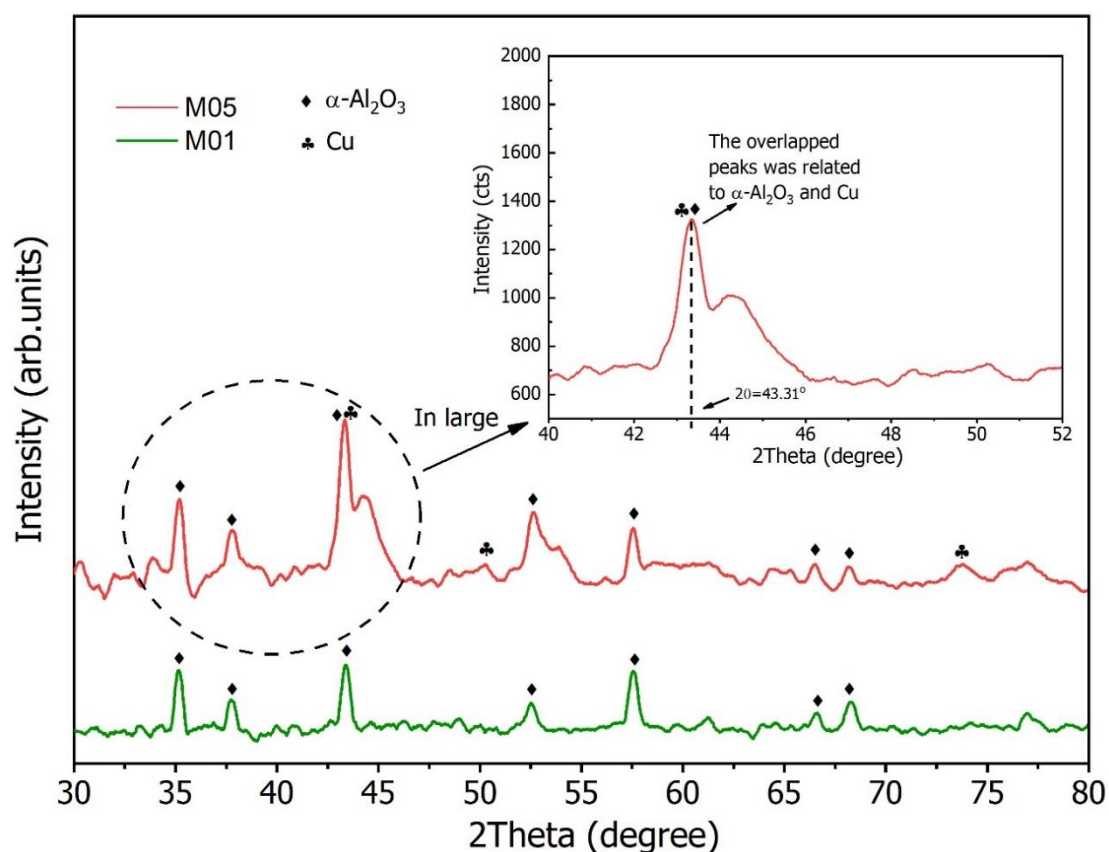


Fig. 4. XRD patterns of the M01 and M05 samples were sintered at 1150°C for two hours

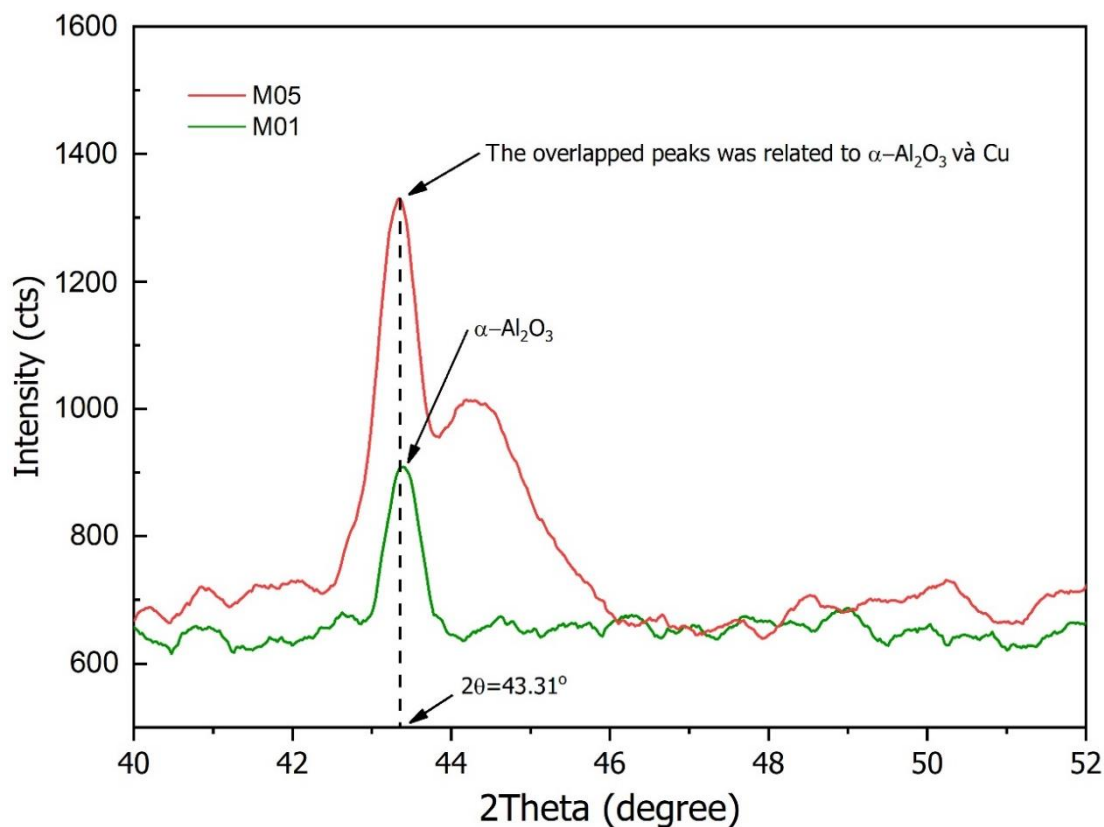


Fig. 5. The overlapped diffraction peak at $2\theta = 43.31^\circ$ was related to α -Al₂O₃ and Cu

Calculation results from formula (1) show that the formed particle has a size of 20.10 nm. This scientific result proves the red color is included in the glaze layer of the M5 sample. When light shines, copper particles less than 20 nm in size will form a surface plasmon effect that makes the red color of the glaze. This red color is especially strong for metals with strong absorption and scattering of visible light, such as gold, silver, and copper [23].

The functional group composition of the M5 sample was also analyzed by the FTIR method. Fig. 6 shows the FT-IR spectrum of the M05 sample. On the FTIR spectrum, there are characteristic peaks for bending vibration of the Cu-O bond in Cu_2O at 613.7 cm^{-1} and 654.4 cm^{-1} [24-26]. The presence of Cu_2O indicates an incomplete CuO reduction product. In addition, the peak at 1040 cm^{-1} is characteristic of the elastic vibrations of the Si-O bond [10, 27], and the peak at 462 cm^{-1} is typical of the bending vibrations of the O-Si-bond [27]. The vibrations of the O-H group at wave number position 1630 cm^{-1} and the CO_3^{2-} group at wave number

$1457, 1387\text{ cm}^{-1}$ are typical peaks for moist air absorbed by the sample [28]. The vibration of the Si-C at position $782\text{--}825\text{ cm}^{-1}$ was also not found in Fig. 6 [29]. It proves that SiC has fully reacted.

4. CONCLUSIONS

The copper red glaze was formed by adding SiC and CuO additives to a base glaze. Thank to in situ reducing agent SiC, the copper red glaze can be created in an oxidizing kiln atmosphere. The thermal analysis showed that the in situ SiC reducing agent reduces CuO to Cu_2O and Cu in the whole glaze mass in the temperature range of $1000\text{--}1100^\circ\text{C}$, the strongest at 1068°C . The suitable glaze firing temperature is 1150°C . Optical microscopy results show that the glaze using SiC reducing agent adheres well to the surface of the ceramic body. The XRD and FTIR analysis results showed that Cu was formed from CuO . However, this reduction reaction is not complete because Cu_2O is still present. The copper red glaze is due to the surface plasmon effect caused by nano-sized copper particles.

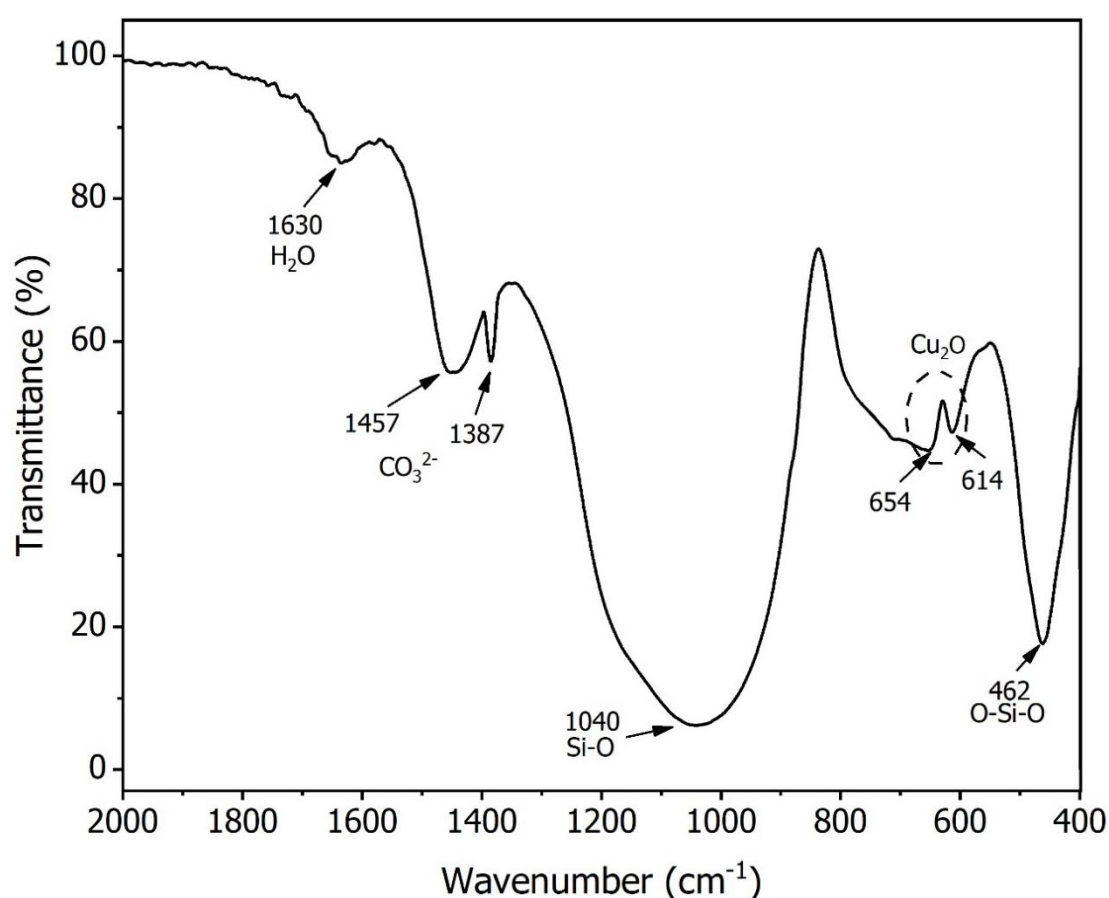


Fig. 6. FT-IR spectrum of the M05 sample

ACKNOWLEDGEMENT

We acknowledge Ho Chi Minh City University of Technology (HCMUT), VNU-HCM for supporting this study.

REFERENCES

- [1]. Jiayu, H. Cui, J. Xingguo, Z. He, L. Gen, L. Hanwen, L. Baoqiang, K. Yong, L. "The birth of copper-red glaze: Optical property and firing technology of the glaze from Changsha Kiln (8th–9th century)," *J. Eur. Ceram. Soc.*, 2022, 42, 1141-1148
- [2]. Jia, C. Li, G. Guan, M. Zhao, J. Zheng, Y. Wang, G. Wei, X. Lei, Y. "A short but glorious porcelain glaze of Early Ming Dynasty: New finding of raw material and colorants in the copper red glaze," *J. Eur. Ceram. Soc.*, 2021, 41, 3809-3815.
- [3]. Colomban, P. "The Use of Metal Nanoparticles to Produce Yellow, Red and Iridescent Colour, from Bronze Age to Present Times in Lustre Pottery and Glass: Solid State Chemistry, Spectroscopy, and Nanostructure." *J. Nano. Res.*, 2009, 8, 109-132.
- [4]. Brown, S.F. Norton, F.H. "Constitution of Copper-Red Glazes." *J. Am. Ceram. Soc.*, 1959, 42, 499-503.
- [5]. Wakamatsu, M. Takeuchi, N. Nagai, H. Ishida, S. "Chemical States of Copper and Tin in Copper Glazes Fired under Various Atmospheres." *J. Am. Ceram. Soc.*, 1989, 72, 16-19.
- [6]. Reinos, J.J. Romero, J.J. Jaquotot, P. Bengochea, M.A. Fernández, J.F. "Copper-based hydrophobic ceramic nanocoating." *J. Eur. Ceram. Soc.*, 2012, 32, 277-282.
- [7]. Leitner, J. Sedmidubský, D. Lojka, M. Jankovský, O. "The Effect of Nanosizing on the Oxidation of Partially Oxidized Copper Nanoparticles." *Materials*, 2020, 13, 2878.
- [8]. Kim, S.H. Magkiriadou, S. Rhee, D.K. Lee, D.S. Yoo P.J. Manoharan, V.N. Yi, G.R. "Inverse Photonic Glasses by Packing Bidisperse Hollow Microspheres with Uniform Cores." *ACS Appl. Mater. Interfaces*, 2017, 9, 24155-24160.
- [9]. Zhu, C. Wu, X. Zhu, X. Wang, Y. Liu, X. Li, J. Zheng, Z. "Preparation of copper-red glazes by in-situ reductive process and its coloring research." *J. Ceram. Soc. Jpn.*, 2017, 125, 584-587.
- [10]. Baggs, A.E. Littlefield, E. "The production and control of copper reds in an oxidizing kiln atmosphere." *J. Am. Ceram. Soc.*, 1932, 15, 265-272.
- [11]. Para, P. Kholam, W. Duangchuen, A. Uarsilp, W. Sriprang, N. Namahoot, J. Mopoung, S. "Low firing Zn metallic composite glazes for earthenware." *India J. Sci. Technol.*, 2017, 10, 1-10.
- [12]. Zhu, C. Wang, Y. Lu, Q. Zhao, H. Zhu, X. Fa, W. Zheng, Z. "Reproduction of Jun-red glazes with nano-sized copper oxide." *J. Am. Ceram. Soc.*, 2017, 100, 4562 - 4569.
- [13]. Xudan, D. Meng, W. Rui, Z. Keke, G. Bingbing, F. Weimin, L. Jia, M. Hongsong, Z. "Crucial effect of SiC particles on in situ synthesized mullite whisker reinforced Al₂O₃-SiC composite during microwave sintering." *Process. Appl. Ceram.*, 2017, 11, 106-112.
- [14]. Qin, D. Shen, C. Wang, H. Guan, L. Zhang, R. "Preparation of SiC-SiO₂-CuO composites." *J. Mater. Sci.*, 2007, 42, 7457-7460.
- [15]. Zhu, J. Shi, P. Wang, F. Zhao, T. "Preparation of the moon-white glaze by carbothermic reduction of Fe₂O₃ and SiC." *J. Eur. Ceram. Soc.*, 2015, 35, 4603-4609.
- [16]. Li, Y. Yang, Y. Zhu, J. Zhang, X. Jhang, S. Zhang, Z. Yao, Z. Solbrekken, G. "Colour-generating mechanism of copper-red porcelain from Changsha Kiln (A.D. 7th–10th century), China." *Ceram. Int.*, 2016, 42, 8495.
- [17]. Minh, D.Q. Linh, N.T.T. Quyen, P.V.T.H. Thang, N.H. "The Novel Crystalline Glaze for Decoration of Ceramic Pottery." *Mater. Sci. Forum*, 2020, 987, 165-170.
- [18]. Xue, J. Zhong, J. Mao, Y. Xu, C. Liu, W. Huang, Y. "Effect of CuO on crystallisation and properties of red R₂O–CaO–MgO–Al₂O₃–SiO₂ glass-ceramics from granite wastes." *Ceram. Int.*, 2020, 46, 23186-23193.
- [19]. Patterson, A.L. "The Scherrer Formula for X-Ray Particle Size Determination." *Phys. Rev.*, 1939, 56, 978.
- [20]. Yamaguchi, N. Masuda, Y. Yamada, Y. Narusawa, H. Han-Cheol, C. Tamaki, Y.

- Miyazaki, T. "Synthesis of CaO-SiO_2 Compounds Using Materials Extracted from Industrial Wastes." *Open J. Inorg. Non-Met. Mater.*, 2015, 05, 1-10.
- [21]. Eo, H.J. Lee, B.H. "Analysis of the Coloration Characteristics of Copper Red Glaze Using Raman Microscope." *J. Korean Ceram. Soc.*, 2013, 50, 518.
- [22]. Zhu, H. Zhang, C. Yin, Y. "Novel synthesis of copper nanoparticles: influence of the synthesis conditions on the particle size." *Nanotechnology*, 2005, 16, 3079.
- [23]. Cavalcante, P.M.T. Dondi, M. Guarini, G. Raimondo, M. Baldi, G. "Colour performance of ceramic nano-pigments." *Dyes Pigm.*, 2009, 80, 226-232.
- [24]. Ho, W.C. Tay, Q. Qi, H. Huang, Z. Li, J. Chen, Z. "Photocatalytic and Adsorption Performances of Faceted Cuprous Oxide (Cu_2O) Particles for the Removal of Methyl Orange (MO) from Aqueous Media." *Molecules*, 2017, 22, 677.
- [25]. Nikabadi, H.R. Shahtahmasebi, N. Rokn-Abadi, M.R. Karimipour, M. Mohagheghi, M.M.B. "Structural verification and optical characterization of $\text{SiO}_2\text{-Au-Cu}_2\text{O}$ nanoparticles." *Bull. Mater. Sci.*, 2014, 37, 527-532.
- [26]. Kansal, I. Goel, A. Tulyaganov, D.U. Rajagopal, R.R. Ferreira, J.M.F. "Structural and thermal characterization of $\text{CaO-MgO-SiO}_2\text{-P}_2\text{O}_5\text{-CaF}_2$ glasses." *J. Eur. Ceram. Soc.*, 2012, 32, 2739-2746.
- [27]. Partyka, J. Sitarz, M. Leśniak, M. Gasek, K. Jeleń, P. "The effect of $\text{SiO}_2/\text{Al}_2\text{O}_3$ ratio on the structure and microstructure of the glazes from $\text{SiO}_2\text{-Al}_2\text{O}_3\text{-CaO MgO-Na}_2\text{O-K}_2\text{O}$ system." *Spectrochim. Acta. Part. A*, 2015, 134, 621-630.
- [28]. Meng, X. Li, Z. Yun, N. Zhang, Z. "A Comparison of Pd^0 Nanoparticles and Pd^{2+} Modified $\text{Bi}_2\text{O}_3\text{CO}_3$ for Visible Light-Driven Photocatalysis." *J. Nanotechnol.*, 2018, 2018, 1-9.
- [29]. Minh, D.Q. Khai, T.V. Minh, H.N. Nhi, N.V.U. Kien, K.D.T. "Effect of composition on the ability to form $\text{SiC/SiO}_2\text{-C}$ composite from rice husk and silica gel." *J. Ceram. Process. Res.*, 2021, 22, 246-251.